SINTER DENSIFICATION OF NANOCRYSTALLINE COMPOSITE W-CU POWDER

F. Alves da Costa*, F. Ambrozio Filho, N. Batista de Lima**, U. Umbelino Gomes***, C. Alves Jr.***, Vaclav Hajek***, Angelus G.P. da Silva**** and Daniel Rodrigues*******

High-energy ball milling (HEBM) was used to prepare composite W-30 w/o Cu powder consisting of well-dispersed nanometer-sized tungsten particles in a copper matrix. Densification of compacts sintered at two heating rates (7.6°C and 10°C/min), below and above the melting point of copper, was monitored. Optical and electron metallography and X-ray diffraction were utilized to characterize microstructures, to determine the tungsten and copper grain sizes, and to identify constituents in the sintered samples. A density of about 72% at the pore-free level was obtained by solid-state sintering. Tungsten and copper nanocrystals were observed to grow as temperature and time increased. The growth of nanometer-sized particles of tungsten inside the composite particles was also detected. Copper spread before reaching its melting point, filling pores between the composite powder particles. Sintering at 1,200°C for 60 min resulted in a final density of about 95% of the pore-free level, with an attendant homogeneous microstructure.

INTRODUCTION

Pseudo-alloys based on the tungsten-copper system are widely used in the electromechanical industry, primarily as electrical contacts and welding electrodes. Important properties are a high electrical and thermal conductivity, a high resistance to arc-discharge erosion, and a low thermal-expansion coefficient.[1,2] Attendant attractive thermal properties and a high microwave-absorption capability enhance the potential use of tungsten-copper alloys for heat spreaders and semiconductor devices.[3,4]

Infiltration of liquid copper into the pores of a pre-sintered porous tungsten substrate, or the liquid-phase sintering of mixed tungsten and copper powders are techniques commonly employed to produce thermal-management materials. However, these processes exhibit intrinsic limitations. Tungsten skeletons with complex geometries are difficult to fill with liquid copper, and attempting to do so often results in heterogeneous infiltration and distribution of the copper. Post-processing treatments are necessary to eliminate, or to largely suppress, porosity and internal heterogeneity. Liquid-phase sintering of tungsten and copper compacts also fails to achieve dense and homogeneous structures because of mutual insolubility of the components, and the low wettability of tungsten by liquid copper.[5-8] The addition of small amounts of cobalt, nickel, palladium, or iron can increase the sinter-

Doctoral Student, **Professor, Instituto de Pesquisas Energeticas e Nucleares, Laboratório de Metalurgia do Pó, IPEN, Av. Prof. Lineu Prestes 2242, Cidade Universitária, 05508-000, São Paulo, SP, Brazil, ***Professor, Departamento de Física Teórica e Experimental, Universidade Federal do Rion Grande do Norte, Campus Universitário, 59072-970, Natal, RN, Brazil, umbelino@dfte.ufrn.br, ****Professor, Laboratório de Materiais Avançados, Universidade Estadual do Norte Fluminense, 28015-620, Campos de Goytacazes, RJ, Brazil, *** Professor, Laboratório de Metalurgia do Pó e Materiais Magnéticos, IPT, 05508-901, Cidade Universitária, São Paulo, SP, Brazil*

ability of mixed tungsten-copper powder compacts.[9–13] These elemental additions contribute to an increase in density, but with an attendant decrease in the electrical and thermal conductivity of the copper matrix.[14]

Homogeneous tungsten-copper composites, with a density approaching the pore-free level, can be obtained by the liquid-phase sintering of a pre-alloyed nanocrystalline (NC) tungsten-copper powder. A well-dispersed tungsten component in the copper matrix is established by high-energy ball milling (HEBM), also termed mechanical alloying.[15–19] Furthermore, the sintering temperature is lower than that required for the liquid-phase sintering of conventionally prepared tungsten-copper powder mixtures, and sintering below the melting point of copper yields a material with acceptable density.[20,21]

In the present work, the sintering behavior of a NC W-30 w/o Cu composite powder, prepared by HEBM, was monitored, below and above the melting point of copper. The sintered compacts were evaluated as a function of heating rate, sintering temperature, and isothermal time, in terms of microstructural characteristics.

EXPERIMENTAL PROCEDURE

Tungsten powder, with an average particle size of 0.78 mm, was obtained from Wolfram GmbH, Austria, Figure 1(a). Atomized copper powder, with an average size of 28 μm, was supplied by Metalpó Indústria e Comércio Ltda., Brazil, Figure 1(b). The tungsten-copper composite powder with 30 w/o copper was prepared by HEBM in a Fritsch Pulverisette 7 planetary mill. Milling was performed in dry air for 51 h, using four WC-balls 14.8 mm dia with a total weight of 100 g and a ball: powder ratio of 10:3 by weight.

Cylindrical samples 9.7 mm in dia x 2.1–2.6 mm in height were prepared by single-action uniaxial compaction at 210 MPa. The green density (d_i) of the NC W-30 w/o Cu composite powder was 61 ± 1% of the theoretically calculated pore-free density (d_t). Compacts were sintered in a resistance furnace in a hydrogen atmosphere; sintering conditions are given in Table I. The sintering temperature was measured using a thermocouple in contact with the sample inside the furnace.

The green density (d_i) and the sintered density (d_f) were measured by the geometric method (weight/volume) and the percent densification (d) was then calculated from the relation:

$$d = \left| \frac{d_f - d_i}{d_t - d_i} \right| \times 100 \qquad (1)$$

The morphologies, particle sizes, and particle-size distributions, of the tungsten and copper powders were characterized by optical microscopy (OM), and by scanning electron microscopy (SEM). These techniques were also used to monitor the cross section of sintered samples. Possible contamination resulting from HEBM was examined by energy-dispersive X-ray (EDX) analysis. X-ray diffraction (XRD) was utilized to identify the phases present, and to determine the tungsten and copper grain sizes.

TABLE I. Sintering Conditions for NC W-30 w/o Cu Compacts

Compact Number	Heating rate (°C/min)	Temperature (°C)	Time at Isotherm (min)
1	10	930	0
2	7.6	1045	0
3	7.6	1095	0
4	7.6	1145	0
5	10	1200	60

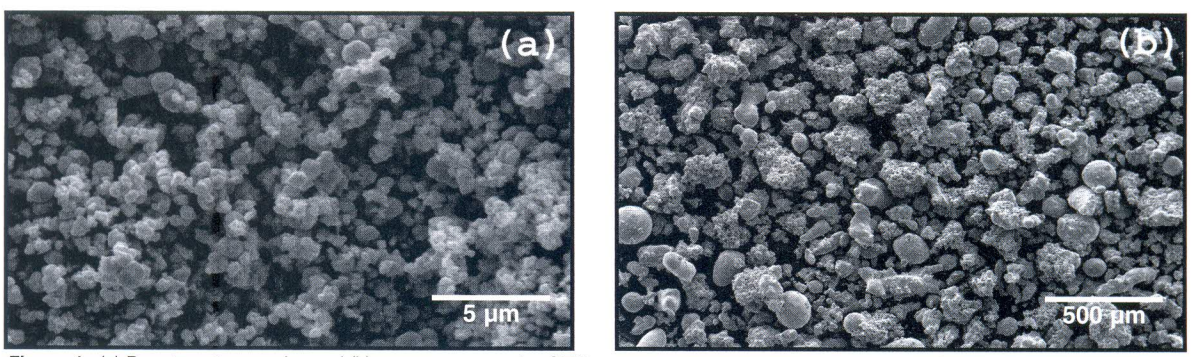

Figure 1. (a) Pure tungsten powder, and (b) pure copper powder. SEM

The mean grain size D of the tungsten and copper was calculated from the relation:[22]

$$D = \frac{0.9\lambda}{B\cos\Theta} \quad (2)$$

where λ is the wavelength of the x-radiation (0.154 nm for CuKα), θ is the diffraction angle, and B is the full width at half maximum (FWHM) of the diffraction peak.

RESULTS AND DISCUSSION

Powder Characteristics of HEBM Powder

Particle shape, particle size and the particle-size-distribution change during HEBM, since the high-energy impact of the WC balls repeatedly deforms, cold welds and fractures the particles. During HEBM, the hard brittle tungsten is reduced to nanometer size and is dispersed in the soft ductile copper matrix. HEBM continues until the composite particle size and shape reach equilibrium, and the tungsten particles are homogeneously dispersed in the copper matrix. The composite particle size increases, exceeding that of the original tungsten and copper particles, Figures 2(a) and 2(b). At equilibrium, the original tungsten particles and copper particles can no longer be resolved. This confirms that the tungsten particles have been refined to a size < 300 nm, the limit of resolution of the SEM used.

The XRD image confirms the presence of tungsten and copper diffraction peaks, Figure 3. Thus, the metal components in the composite powder remained crystalline and did not form an amorphous phase. However, a broadening and shift of the tungsten and copper peaks were detected, Figure 4. Table II summarizes the calculated

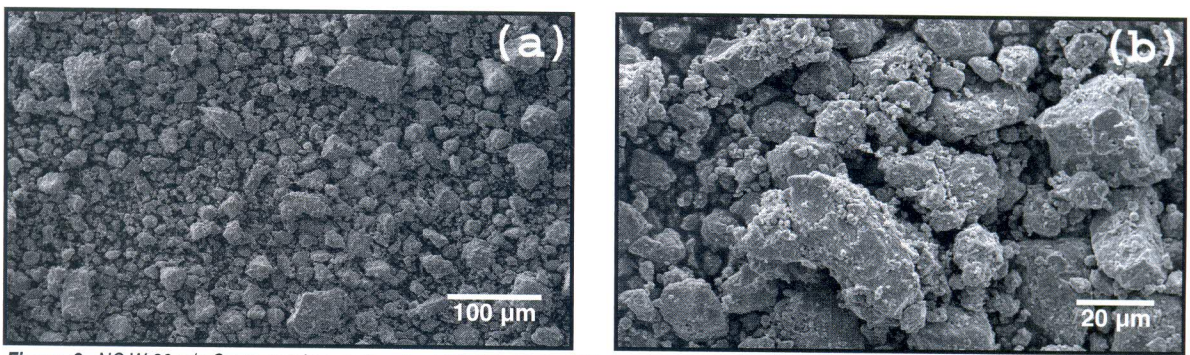

Figure 2. NC W-30 w/o Cu composite powder after HEBM for 51 h. SEM

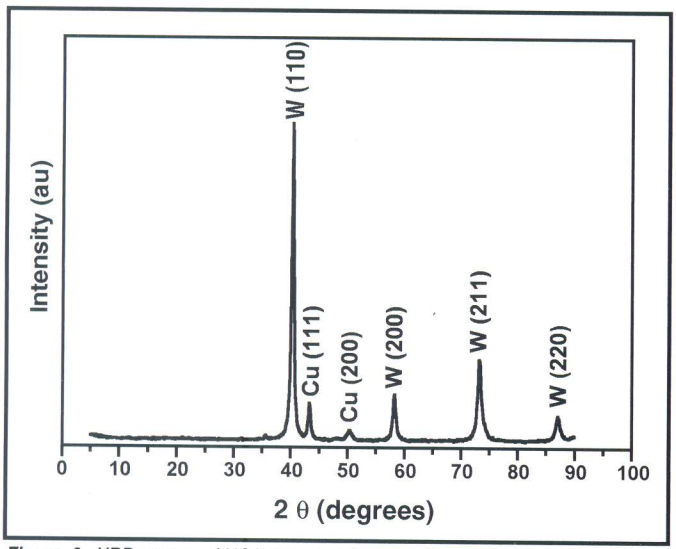

Figure 3. XRD pattern of NC W-30 w/o Cu composite powder

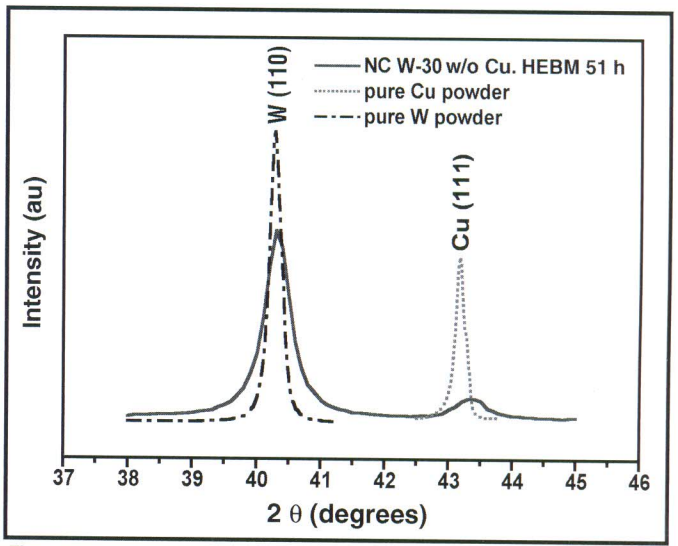

Figure 4. Broadening and shift of tungsten (110) and copper (111) peaks of NC W-30 w/o Cu composite powder

TABLE II. Calculated Grain Sizes of HEBM Tungsten, Copper, and NC W-30 w/o Cu Powders and Sintered Compact No. 5

Powder or Sintered Compact	θ_W* (°)	θ_{Cu}** (°)	B_W*** (°)	B_{Cu}**** (°)	D_W (nm)	D_{Cu} (nm)
W	20.14	-	0.24	-	35.3	-
Cu	-	21.58	-	0.19	-	45
NC W-30 w/o Cu	20.16	21.6	0.48	0.7	18	12
Sample 5	20.08	21.61	0.3	0.36	28.2	23.8

* Position of $(110)_w$ peak. ** Position of $(111)_{Cu}$ peak. ***Width of $(110)_w$ peak. **** Width of $(111)_{Cu}$ peak.

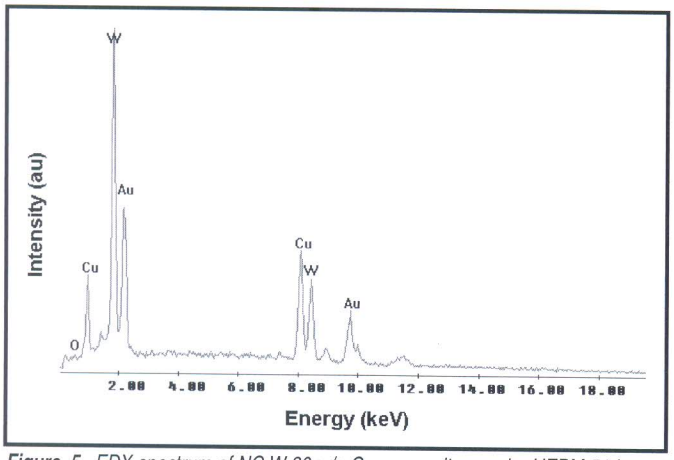

Figure 5. EDX spectrum of NC W-30 w/o Cu composite powder HEBM 51 h

copper and tungsten grain sizes of the starting powder, and of the resulting composite powder. During HEBM, the copper and tungsten grain sizes decreased to 12 nm and 18 nm, respectively, forming nanocrystalline NC W-30 w/o Cu powder. EDX analysis of the NC W-30 w/o Cu powder composite did not reveal any contamination/oxidation as a result of HEBM, Figure 5. The diffraction peaks of the gold originated from sample preparation.

Effect of Sintering on Properties and Microstructure

Figure 6 shows the variation in the relative sintered density and densification of each sintered NC W-30 w/o Cu compact, as a function of the sintering temperature. A densification of about 11% and a relative density of approximately 72% of the pore-free value were attained during solid-state sintering of the NC W-30 w/o Cu compacts at 1,045°C. A significant increase in densification of ~ 18% was detected between compacts no. 2 and no. 3, which were sintered below (1,045°C) and above (1,095°C) the melting point of the copper (1,083°C). This difference is attributed to particle-enhanced rearrangement as the temperature approaches the melting point of the copper. The highest densification of ~ 33%, and an attendant relative density of ~ 95% of the pore-free level, were attained in compact no. 5, which was sintered at 1,200°C for 1 h.

The microstructure of compact no. 1 sintered at 930°C, but which was not held at the isotherm, showed composite particles of the same size and shape as the initial particles, albeit separated by voids, Figures 7(a) and 7(b). The tungsten particles inside the composite particles were small and difficult to resolve, although some of the less-refined particles were still visible, Figure 7(b). The tungsten particles were found to grow when the sintering temperature was increased to 1,045°C, as shown in Figures 8(a) and 8(b). These micrographs also show copper flowing out of the composite particles, and beginning to fill the voids. This process is responsible for the higher densification (about 11%) of the NC W-30 w/o Cu composite achieved during solid-phase sintering. Similar results were reported by Ryu et al.[20] and Lee & Kim.[23] Figures 9(a) and 9(b) show the microstructure of compact no.3 sintered at 1,095°C with zero time at the isotherm. This microstructure is similar to that of compact no. 2 sintered at 1,045°C, except that growth of the tungsten inside the composite parti-

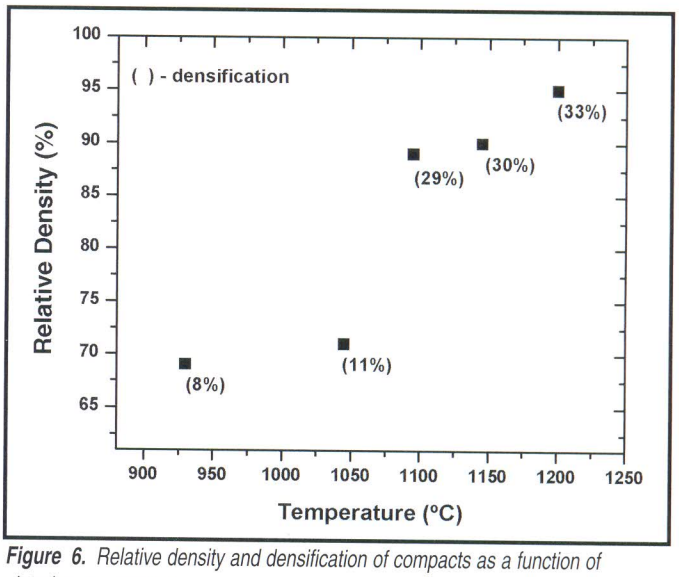

Figure 6. Relative density and densification of compacts as a function of sintering temperature

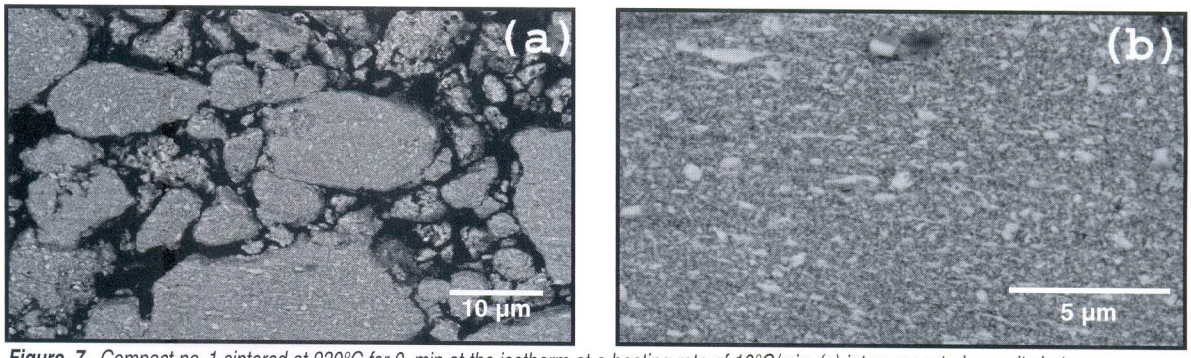

Figure 7. Compact no. 1 sintered at 930°C for 0 min at the isotherm at a heating rate of 10°C/min. (a) interconnected porosity between composite powder particles, and (b) internal region of composite particle. SEM

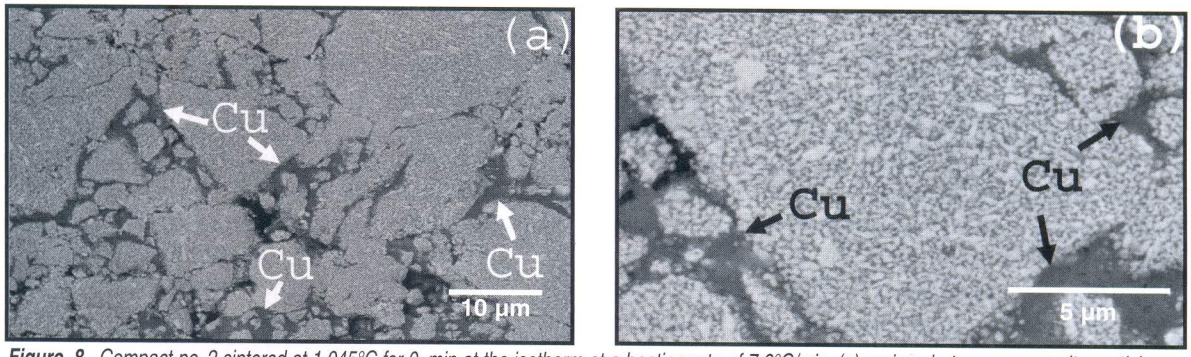

Figure 8. Compact no. 2 sintered at 1,045°C for 0 min at the isotherm at a heating rate of 7.6°C/min. (a) regions between composite particles filled with copper, and (b) spreading of copper, and growth of embedded nanometer-sized particles of tungsten inside composite particles. SEM

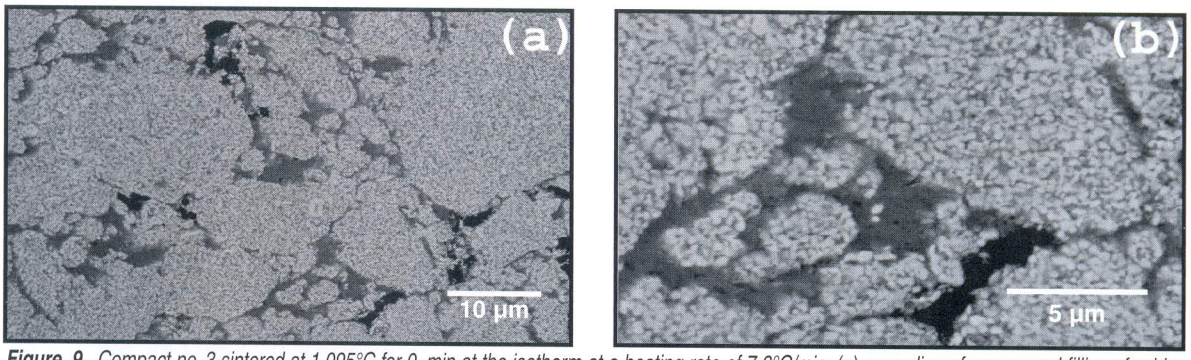

Figure 9. Compact no. 3 sintered at 1,095°C for 0 min at the isotherm at a heating rate of 7.6°C/min. (a) spreading of copper and filling of voids between composite particles, and (b) copper pools, and growth of embedded nanometer-sized tungsten particles inside composite particles. SEM

cles is more pronounced, and the voids are essentially filled by copper.

The migration of copper from inside the NC composite particles at a temperature below its melting point should result in a rearrangement of particles during solid-state sintering. The sintered structure can be attributed to two different sintering mechanisms:

(i) coalescence of nanometer-sized tungsten particles inside the composite particles. As the tungsten particles grow, they form an interconnected skeleton which begins to shrink as the temperature rises. This reduces the spacing of the tungsten particles and forces the copper out, even below its melting point.

(ii) sintering of the composite particles due to the migration of copper to the particle sur-

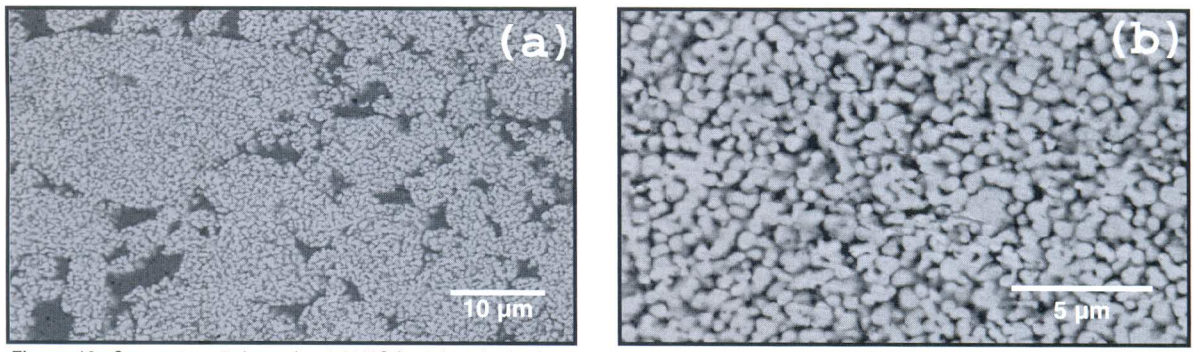

Figure 10. Compact no. 5 sintered at 1,200°C for 1 h at the isotherm at a heating rate of 10°C/min. (a) well-dispersed copper and low density of voids between composite particles, and (b) internal region of composite particle with increased size of embedded nanometer-sized particles of tungsten. SEM

faces, thereby filling the voids by capillarity. This results in significant densification of the NC W-30 w/o Cu during solid state sintering.

Figures 10(a) and 10(b) are representative of the microstructure of compact no. 5 sintered at 1,200°C for 1 h at the isotherm. At low magnification (Figure 10(a)), the composite particles retain their size and shape and few voids are visible between the composite particles. The copper is distributed uniformly and a dense structure (relative density ~ 95% of the pore-free level) is attained, Figure 6. At a higher magnification, large tungsten particles are present with an estimated average particle size of 600 nm, Figure 10(b). Kim et al.[15,16] identified two particle rearrangement processes during the liquid-phase sintering of NC W-Cu samples: *(i)* extensive rearrangement of the composite particles during melting of the copper, accompanied by densification, reaching a final density ~ 95% of the pore-free level; and *(ii)* dispersion of the tungsten particles throughout the sample, resulting in structural homogenization and a final density of ~ 97% of the pore-free level. In the present study, the second type of particle rearrangement was not confirmed; the composite particles retained both their original size and shape.

Table II confirms that the tungsten and copper grain sizes of the sintered W-30 w/o Cu (compact no. 5), increase, as expected. However, the grain sizes remain well below the original grain sizes of the tungsten and copper powders.

CONCLUSIONS

1. After HEBM for 51 h, a NC W-30 w/o Cu composite powder is obtained with well-dispersed and refined tungsten particles in a ductile copper matrix.
2. Solid-state sintering, below the melting point of copper, resulted in a relative density ~ 72% of the pore-free level.
3. Sintering in the presence of liquid copper at 1,200°C for 60 min resulted in a relative density ~ 95% of the pore-free level, with retention of the size and shape of the composite particles.
4. With increasing temperature and time at the isotherm, the tungsten and copper nanocrystals grew. Nanometer-sized tungsten particles inside the composite particles also grew.
5. Before reaching its melting point, copper was observed to spread and fill the voids between the composite powder particles.

ACKNOWLEDGEMENTS

The authors are indebted to Metalpó Indústria e Comércio Ltda (Brazil), represented by Eng. Ana Keiko, for its donation of copper powder. Professor J.R. Martinelli and R.M. Rocha, M.Sc., IPEN, performed the laser diffraction particle size measurements, and Dr. Nildemar, IPEN took the SEM images. This work was supported financially by FAPESP, Project: 00/00255-9, Brazil.

REFERENCES

1. C.D. Desforges, "Sintered Materials for Electrical Contacts", *Powder Metallurgy*, 1979, vol. 22, no. 3, pp. 138–144.
2. N.C. Kothari, "Factors Affecting Tungsten-Copper and Tungsten-Silver Electrical Contact Materials", *Powder Metall. Int.*, 1982, vol. 14, no. 3, pp. 139–143.
3. R.M. German, K.F. Hens and J.L. Johnson, "Powder

Metallurgy Processing of Thermal Management Materials for Microelectronic Applications", *Int. J. Powder Metall.*, 1994, vol. 30, no. 2, pp. 205–215.

4. J.L. Sepulveda and D.E. Jech, "Functionally Graded Copper/Tungsten Metal Composites", *Proc. of Powder Metallurgy World Congress*, compiled by K. Kosuge and H. Nagai, Japan Society of Powder and Powder Metallurgy, Kyoto, Japan, 2000, vol. 2, part 2, pp. 1,461–1,464.
5. J. Lezanski and W. Rutkowski, "Infiltration of a Liquid in Sintered Tungsten—Three Stages of Infiltration", *Powder Metall. Int.*, 1987, vol. 19, no. 2, pp. 29–31.
6. A. Upadhyaya and R.M. German, "Densification and Dilation of Sintered W-Cu Alloys", *Int. J. Powder Metall.*, 1998, vol. 34, no. 2, pp. 43–55.
7. F.A. Costa, "Estudo da Sinterização de Ligas de W-Cu", 2000, M.S. Thesis, Programa de Pós-Graduação em Engenharia Mecânica, Universidade Federal do Rio Grande do Norte, Natal, Brazil.
8. U.U. Gomes, F.A. Costa and A.G.P. Silva, "On Sintering of W-Cu Composite Alloys", *Proc. of the 15th International Plansee Seminar*, compiled by G. Kneringer, P. Rödhammer and H. Wildner, Plansee Holding AG, Reutte, Tyrol, Austria, 2001, vol. 1, part 24, pp. 177–189.
9. I.H. Moon and J.S. Lee, "Activated Sintering of Tungsten-Copper Contact Materials", *Powder Metallurgy*, 1979, vol. 22, no. 1, pp. 5–7.
10. F. Dore, C.H. Allibert, R. Baccino and J.F. Lartigue, "Effects of the Phase Size and of Fe Additions on the Sintering Behaviour of Composite Powder W-Cu (20wt%)", ibid. reference no. 8, vol. 1, part 12, pp. 81–93.
11. P.E. Zovas, R.M. German, K.S. Hwang and C.J. Li, "Activated and Liquid-Phase Sintering—Progress and Problems", *J. of Metals*, 1983, vol. 35, pp. 28–33.
12. J.L. Johnson and R.M. German, "Chemical Activated Liquid-Phase Sintering of Tungsten-Copper", *Int. J. Powder Metall.*, 1994, vol. 30, no. 1, pp. 91–102.
13. S. Lee, M-H. Hong, J-W. Noh, W.H. Baek and B-S. Chun, "A Study on the Sintering Behavior of Co-reduced W-Cu Composite Powder Containing Transition Elements", ibid. reference no. 4, vol. 1, part 1, pp. 686–689.
14. J.L. Johnson and R.M. German, "A Theory of Activated Liquid-Phase Sintering and Its Application to the W-Cu System", *Advances in Powder Metallurgy & Particulate Materials*, compiled by J.M. Capus and R.M. German, Metal Powder Industries Federation, Princeton, NJ, 1992, vol. 3, pp. 35–46.
15. J-C. Kim, S-S. Ryu, Y.D. Kim and I-H. Moon, "Densification Behavior of Mechanically Alloyed W-Cu Composite Powders by the Double Rearrangement Process", *Scripta Mater.*, 1998, vol. 39, no. 6, pp. 669–676.
16. J-C. Kim, S-S. Ryu, H. Lee and I-H. Moon, "Metal Injection Molding of Nanostructured W-Cu Composite Powder", *Int. J. Powder Metall.*, 1999, vol. 35, no. 4, pp. 47–55.
17. F.A. Costa, F. Ambrózio Filho, A.G.P. Silva and U.U. Gomes, "Efeito da Moagem de Alta Energia, Realizada em Moinho Planetário, na Sinterização do Compósito W-Cu", *II National Congress of Mechanical Engineering*, compiled by J.A. Riul and M.A.W. Cavalcanti, Universidade Federal da Paraíba, João Pessoa, PB, 2002, CD-ROM.
18. B.K. Kim and S.H. Hong, "Densification of W/Cu Nanocomposite," ibid. reference no. 4, vol. 1, part 1, pp. 682–685.
19. D.G. Kim, W-S. Shim, J.S. Kim, Y.D. Kim and I-H. Moon, "Fabrication of W-Cu Nanocomposite by Reduction of WO_3-CuO," ibid. reference no. 8, vol. 1, part 10, pp. 61–67.
20. S.S. Ryu, Y.D. Kim and I.H. Moon, "Dilatometric Analysis on the Sintering Behavior of Nanocrystalline W-Cu Prepared by Mechanical Alloying," *J. of Alloys and Compounds*, 2002, vol. 335, pp. 233–240.
21. J-C. Kim and I-H. Moon, "Sintering of Nanostructured W-Cu Alloys Prepared by Mechanical Alloying", *Nanostruct. Mater.*, 1998, vol. 10, no. 2, pp. 283–290.
22. B.D. Cullity, *Elements of X-ray Diffraction*, 1978, Addison Wesley Publishing Company, Reading, MA, USA.
23. J.S. Lee and T.H. Kim, "Densification and Microstructure of the Nanocomposite W-Cu Powders," *Nanostruct. Mater.*, 1995, vol. 6, pp. 691–694.